sustainability

MDPI

Article

Reflective Properties and Lighting Quality of Urban Asphalt Roads in a Full-Service Cycle: A Longitudinal Study in Zhejiang Province, China

Chi Zhang [1,2], Chuan Lei [1], Lei Ye [3], Cheng Kang [1,2,4], Meihong Wang [5], Zhiyi Huang [1] and Ke Wu [1,2,6,*]

1 Key Laboratory of Offshore Geotechnics and Material of Zhejiang Province, Zhejiang University, Hangzhou 310058, China
2 Center of Balance Architecture, Zhejiang University, Hangzhou 310007, China
3 Construction Management Division, Department of Transportation of Zhejiang Province, Hangzhou 310007, China
4 China Railway First Survey and Design Institute Group Co., Ltd., Xi'an 710043, China
5 College of Quality and Safety Engineering, China Jiliang University, Hangzhou 310018, China
6 The Engineering Research Center of Oceanic Sensing Technology and Equipment, Ministry of Education, Zhejiang University, Hangzhou 310058, China
* Correspondence: wuke@zju.edu.cn

Abstract: To optimize the lighting design of urban roads in China and improve traffic safety, the present study conducted a 10-year longitudinal experiment on urban asphalt roads in Zhejiang Province, China, and analyzed variations of the road surface's reflective properties and lighting quality with different service lengths, surface areas, and observation angles. The results showed that these roads were R2 roads with low resilience and strong directional reflection. The average luminance coefficient $Q0$ reached maximum and minimum at the beginning and after around one year of service, respectively. After four years of service, $Q0$ was about 80% of its initial value and remained stable. The specularity factor $S1$ reached a maximum of around two years of service. The average luminance L_{av} was approximately 35%, and overall luminance uniformity U_0 was 31%, lower than that of R3 roads during the toughest period of the service life. If the lighting design follows the 1° observation angle r-table recommended by the specification, high L_{av} and low U_0 occur for roads like expressways, leading to a significant increase in traffic safety risks; collector roads may suffer from insufficient L_{av}. Urban asphalt roads in Zhejiang Province, China, should use the R2 road standard and increase the design value of L_{av} by 35–45%, and high-level roads should increase the design value of U_0 by 40%. The present study will provide scientific references for the design of lighting for urban roads in China, thus promoting long-term sustainable traffic safety in cities.

Keywords: Chinese urban roads; reflective properties of road surface; full-service cycle; lighting quality; observation angle; risk assessment; sustainable safety

check for updates

Citation: Zhang, C.; Lei, C.; Ye, L.; Kang, C.; Wang, M.; Huang, Z.; Wu, K. Reflective Properties and Lighting Quality of Urban Asphalt Roads in a Full-Service Cycle: A Longitudinal Study in Zhejiang Province, China. *Sustainability* **2023**, *15*, 16784. https://doi.org/10.3390/su152416784

Academic Editors: Hui Liu, Longxing Yu, Fuqiang Yang and Chao Chen

Received: 24 October 2023
Revised: 4 December 2023
Accepted: 6 December 2023
Published: 13 December 2023

1. Introduction

More than 50% of road traffic accidents happen at night [1]. Good road lighting quality can reduce night-time traffic injury accidents by 30%, fatal accidents by 64%, and property damage accidents by 17% [2]. The quality of road lighting is influenced significantly by the luminance of the road surface. Road surfaces can absorb and reflect light that falls on them. The luminance of the road surface refers to the intensity of reflected light that the human eye perceives at a specific observation angle. Therefore, the reflective properties of the road surface play a vital role in determining both its luminance and luminance distribution.

The reflective properties of the road surface represent the road surface's capacity to reflect light from various incident angles. In the 1980s, the International Commission on Illumination (CIE) and the Permanent International Association of Road Congresses (PIARC) jointly established a classification system using the average luminance coefficient

($Q0$) and the specular factor ($S1$) to describe the reflectivity and specularity of the road surface, respectively. According to the intensity of the specularity, the roads are divided into four types, i.e., R1, R2, R3, and R4. On this basis, the CIE proposed the standard reduced-luminance coefficient tables (standard *r*-tables) of each type of road and the corresponding standard $Q0$ and $S1$ values ($Q0_{\text{standard}}$ and $S1_{\text{stardard}}$) [3,4]. The CIE road surface reflection classification system has been widely used around the world. For example, the standard *r*-table for the R3 road is used in China to represent the reflective properties of asphalt pavements [5,6].

However, it is worth noting that the classification system proposed by the CIE for road surface reflectance has quite a long history of approximately 40 years. With the rapid development of the design, construction, and material technology for asphalt pavement, the reflective properties of the road surface change as well [7]. In 2007, Chain tested $S1$ and $Q0$ of the asphalt pavement in France and found that $S1$ was between 0.45 and 0.9 and the road belonged to R2 or R3 roads [8]. But, the $Q0$ of these pavements ranged from 0.052 to 0.09, with a difference of −25.7% to 28.6% from the $Q0_{\text{standard}}$ of R2 or R3 roads. And, the difference between the actual average luminance of the road surface and the result calculated according to the standard $Q0_{\text{standard}}$ reached 50%. In 2019, Gildlund conducted measurements of $Q0$ and $S1$ on 138 road surface samples from Switzerland, France, and Finland [9]. Most of the measurements were found to be significantly different from the standard values of the CIE road surface reflection classification system. For instance, most of the measured $Q0$ of the R2 roads were 0.03~0.046 and 0.89~0.17, with a maximum difference of more than 70% from the $Q0_{\text{standard}}$ of R2 roads. If the standard *r*-tables recommended by the CIE are still adopted to calculate the luminance of the road surface, the difference between the average luminance (L_{av}) and the actual measurement results, and between the longitudinal luminance uniformity (U_{L}) and the actual measurement results, is 43.6% and 50%, respectively.

The reduction in the luminance level of the road surface will increase the reaction time of the driver and thus increase the potential risk of a traffic accident [10,11]. Additionally, low overall luminance uniformity on road surfaces results in a substantial difference between the darkest area's luminance and the road surface's average luminance. Since the human eye's adaptation depends on the average luminance, drivers usually face more challenges in detecting dangerous obstacles within the darkest areas when they adapt to a higher average luminance, thus increasing the possibility of collision accidents [12]. Therefore, the CIE standard *r*-tables, $Q0_{\text{standard}}$ and $S1_{\text{stardard}}$, can no longer accurately represent the reflective properties of the current road surface. Consequently, there exists a substantial disparity between the actual lighting quality and safety requirements, which significantly increases the risk to road safety.

Apart from the pavement structure and materials that affect the reflective properties of the road surface, the reflective properties of the pavement also change along its service period due to complex external factors such as service environment and traffic load change. Rice et al. measured *r*-tables of the most commonly used asphalt pavements in the United States under 40 incident angles [13]. They found that the reflectivity of the road surface increased by about 30% after 1.5 years of service, returned to its initial level after 4 years of service, and remained stable later. Nevertheless, Bodmann's 36-month tracking study of the reflective properties of German road surfaces showed that $Q0$ recovered to its initial level and remained stable after one year of service [14]. In addition, Ylinen et al. further explored the impact of wheel crushing on the reflective properties of the road surface in Finland [15]. They collected and measured samples from areas between wheel paths and from areas of the wheel path on the road surface, which had been in use for over two years. Results showed that the maximum difference of $Q0$ and $S1$ between the two areas reached 80% and 73%, respectively. The reflective properties of the wheel path area were similar to those of the standard R2 roads, but the reflective properties of the area between the wheel path were similar to those of standard R1 roads, indicating that the reflectivity and specularity of the wheel path area are stronger. Urban roads in China differ from roads abroad in terms of the construction technology, and have larger traffic volumes and heavier traffic load [16]. However, research on the changes in reflective properties of Chinese urban road pavements over the service life has been scarcely seen.

Additionally, the CIE road surface reflection classification system utilizes 1° as the observation angle α for collecting the reflectance data, which corresponds to a driver's point of view at a height of 1.5 m and a driver's attention area from 60 m to 160 m ahead. But, with the rapid development of urban road construction and vehicle manufacturing technology, the range of the driver's attention area has increased up to 20 m~450 m ahead [17], and the height of vehicles has expanded to 1.4 m~3 m [18]. Meanwhile, due to the need for the seat recline angle [19] and the distance between the driver's eyes and the interior rear-view mirror [20], the height of the driver's viewpoint can reach 1.2 m~2.5 m. As a result, the range of the actual observation angle α for contemporary drivers can be extended to 0.15°~7.12°. Gibbons et al. conducted a measurement of the luminance of road surfaces in Europe, where α was set at 1° to 10° [21]. Their findings demonstrated that increasing α results in an increase in road surface luminance, with a maximum increase of approximately 50%. This is also verified by Strbac-Hadzibegovic et al. [22]. However, according to the European SURFACE project in recent years [23], an increase in α from 1° to 5° resulted in a reduction in the road surface luminance by 50%. In brief, the reflective properties of road surfaces under various observation angles have not reached a consensus, and relevant research on roads in China can be merely seen.

The present study employed a self-constructed measurement platform to gauge the variations in the reflective properties of asphalt pavements with time. Samples of road surfaces from different urban roads located in Zhejiang Province, China, were collected throughout a ten-year service span. DIALux was used to simulate the spatial distribution of luminance of road surfaces with varied service lengths. The present study analyzed the impacts of the observation angle on reflective properties and variation in lighting quality, aiming to provide references for the design of lighting and sustainable safety of urban roads in China.

2. Evaluation System for Reflective Properties

Road surfaces' reflective properties are generally characterized by a set of luminance coefficients, q [12]. q represents the luminance-to-illuminance ratio at a spot on the road surface that is exposed to a single light source. q is influenced by the surface material, the relative positions of the observer, the light source, and the road surface. q can be calculated using Formula (1).

$$q(\alpha, \beta, \gamma) = \frac{L}{E} \tag{1}$$

where α is the angle between the observation direction and the horizontal plane (°), β is the supplementary angle of the angle between the horizontal projection line in the observation direction and the horizontal project of the incident light (°), γ is the angle of incidence measured from the vertical to the direction of illumination (°), L is the luminance of the road surface (cd/m^2), and E is the illuminance on the road surface (lx).

When illuminated from varied directions, the distribution of q does not remain homogenous across all directions, manifesting in an elliptical spatial distribution, as illustrated in Figure 1.

To simplify calculations of road surface luminance, the CIE created a table of luminance coefficient q, which was then converted to reduced-luminance coefficient r, as demonstrated in Equation (2).

$$r(\alpha, \beta, \gamma) = q(\alpha, \beta, \gamma) \cos^3 \gamma \tag{2}$$

Projecting the spatial distribution of r onto the plane with γ = 0° and β = 0° can create a "scattering ellipsoid" (also known as the r projection map) [24]. Figure 2 presents the scattering ellipsoids corresponding with the standard r-table of R1~R4 roads. The size of the scattering ellipsoid indicates the reflectivity of the road surface; larger ellipsoids display a stronger reflection capacity. The flatness of the scattering ellipsoid reflects the specularity of the road surface; the larger the protrusion on the right side, the higher the specularity.

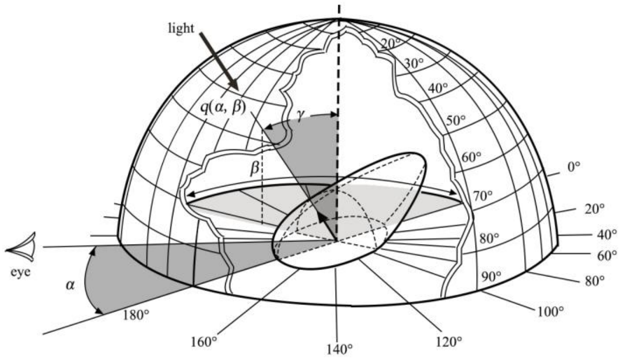

Figure 1. The spatial distribution of the luminance coefficient q.

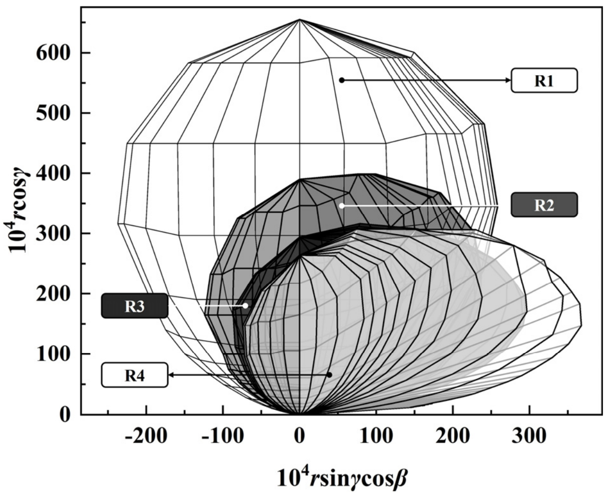

Figure 2. Scattering ellipsoid of the standard r-table of R1~R4 roads.

To assess the reflective properties of a road surface, the CIE also suggests using the evaluation metrics of the average luminance coefficient ($Q0$) and specular factor ($S1$). $Q0$ represents the solid angle-weighted average of q, encompassing a range of 60 m~160 m ahead of the driver at a 1° observation angle. $S1$ is the ratio of two r. The calculation formulas are shown in Equations (3) and (4).

$$Q0 = \frac{\int_0^{\Omega_0} q(\alpha, \beta, \gamma)\mathrm{d}\omega}{\Omega_0} \tag{3}$$

where Ω_0 is the solid angle containing all those directions of light incidence at the point on the road under consideration that are taken into account in the averaging process (°), q is the luminance coefficient (cd/m^2·lx), and ω is the solid angle (°).

$$S1 = \frac{r(0,2)}{r(0,0)} \tag{4}$$

where r (0,2) is the reduced-luminance coefficient at β = 0° and tanγ = 2, and r (0,0) is the reduced-luminance coefficient at β = 0° and tanγ = 0.

3. The Measurement of r and Lighting Simulation

3.1. The Measurement of r

3.1.1. Platform

Figure 3 displays the measurement platform utilized to obtain the reduced-luminance coefficient r, consisting of a light source module, a control module, a measurement module, and a dark room. The light source module comprised a fiber light source and a collimating lens fixed at R = 1 m above the sample via a vertical arm. It projected a collimated beam toward the sample, achieving a collimation accuracy of 0.1°. The control module comprised two motors (motor 1 and motor 2), a vertical arm, a horizontal arm, and a controller. The motors drove the rotation of the horizontal arm, the vertical arm, and the collimating lens. The controller was utilized to manage the motors. The measurement module consisted of the LM-3 luminance meter, the ST520 illuminance meter, and the light-limiting aperture. The LM-3 luminance meter was located at least 2R from the center of the sample and had a measurement field of view of 0.1°. Its observation angle relative to the sample can be adjusted from 0.1° to 10°. The lens of the luminance meter had a 4 mm light-limiting aperture to prevent stray light from entering. The ST520 illuminance meter had a measuring range of 0~80,000 lx. The measurement error for luminance and illuminance was less than 1%. The dark room was built with brackets and black velvet cloths, with a size of 3 m × 3 m × 2 m, and the luminance of the dark indoor environment was lower than 0.001 cd/m^2, meeting the CIE requirements for the testing environment [4].

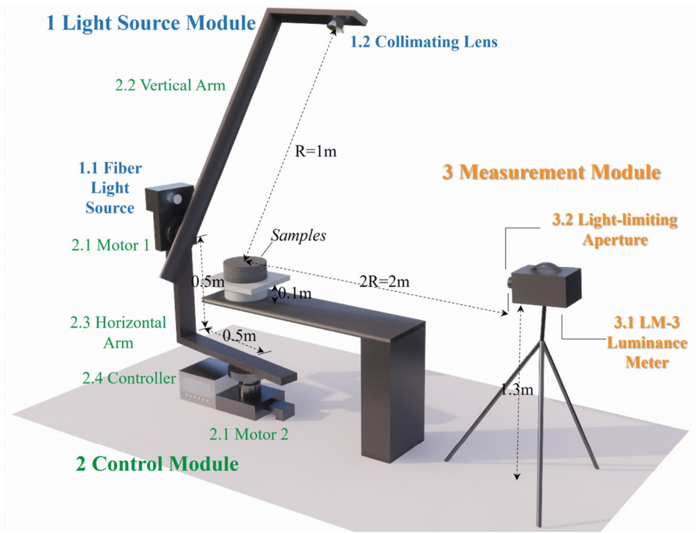

Figure 3. Measurement platform.

3.1.2. Measurement Process and Measured Conditions

Road surface samples were measured using the measurement platform at different service lengths, areas on the road surface, and observation angles α. Initially, the measurement needs to be prepared by adjusting the α between the luminance meter and the road surface sample, activating the collimated light source, and verifying the surface luminance stability of the sample after 30 min. Calibration of the ambient luminance in a dark room is also required. The measurement commences with the control module controlling the collimation light source to sequentially irradiate the sample at 396 incident angles specified in the standard r-table [4]. Meanwhile, the sample's luminance and illuminance are measured using a luminance meter and an illuminance meter, respectively, and the reduced-luminance coefficient r is computed for each incident angle. Finally, once all angles of incidence have been measured and recorded, the measurement platform should be reset and recalibrated before carrying out further measurements.

A total of 5 × 3 × 7 = 105 sets of measured conditions were included for the test, taking the service length of the road, area on the road surface, and observation angle α

into full account. Each set of conditions contains three parallel measured conditions to avoid measurement errors due to individual differences in the road surface samples. The measured conditions are shown in Table 1.

Table 1. The measured conditions.

Length of Service (Year)	Areas on Road Surface	Observation Angle α (°)
0, 1, 2, 3, 4, 6, 8	Curb, Center, Wheel path	0.2, 0.5, 1, 2, 3, 4, 7

3.1.3. Sample Collection

The road surface samples were taken from the urban roads constructed around 2012 in Zhejiang Province. Each test road's samples were categorized into a sample group, as indicated in Table 2.

Table 2. The group of road surface samples.

Sample Group	Sample 1	Sample 2	Sample 3	Sample 4	Sample 5
Road name	Meilin	Binjianger	Qingliu	Linhongdong	Jiangdongwu

The samples were collected from three areas of the road's surface, specifically each test road's edge, center, and wheel path, at various stages throughout its 10-year service life from 2012 to 2022. These stages included 0 year (within 3 months), 1 year, 2 years, 3 years, 4 years, 6 years, and 8 years. The samples obtained in 2012 were collected 2–3 months after the road was built, representing the initial period of the road's service. The connection between the three sampling areas is perpendicular to the direction of travel. The sampling method follows the *Standard Practice for Sampling Bituminous Materials GB/T 11147-2010* [25]. The size of each individual sampling area was 0.3 m × 3 m. Every sample was a cylinder with d = 0.15 m and h = 0.2 m~0.3 m, as specified. Since the sampling process results in wet samples, drying them at a constant temperature before testing is necessary to maintain consistency with the actual road conditions. Figure 4 illustrates the sampling process and partial samples.

(**a**) (**b**)

Figure 4. The sampling process and some samples. (**a**) Sampling process: Sampling preparation (①); Core drilling and sampling (② & ③); Sample extraction (④). (**b**) Showing of the partial samples

3.2. Lighting Simulation

The DIALux light-environment simulation model was established based on the actual lighting conditions of the sampled roads. The lane width is 3.5 m, and the shoulder width is 1.5 m. For lighting, LED lamps with a symmetrical light distribution, a color temperature of 4500 K, a luminous flux of 10,000 lm, an arm length of $H/8$ (where H is the height of the lamp pole, H = 10 m), and an elevation angle of 5° were used.

Three types of *r*-tables were used to simulate the luminance distribution of the road surface: (a) standard *r*-tables, which contain R2 and R3 roads; (b) measured *r*-tables with different service lengths and road areas. The service lengths include 0~8 years. The road surface areas include the edge, center, and wheel path, which are composed according to their original spatial arrangement on the road surface and their respective area proportions of 20%, 60%, and 20%; and (c) Measured *r*-tables with 4 years' service lengths and different road areas were used to simulate the luminance distribution under each observation angle. The road surface areas include the edge, center, and wheel path, which are composed according to their original spatial arrangement on the road surface and their respective area proportions of 20%, 60%, and 20%. The observation angles include 0.2°, 0.5°, 1°, 2°, 3°, 4°, and 7°.

To validate the DIALux light-environment simulation mode's accuracy, the present study compares the calculation results with the field measurements. Following the recommendations in *Lighting Measurement Methods GBT 5700-2008* [26], the field measurements were conducted using an imaging-type luminance meter. The longitudinal area of the measurement was between two lighting poles on the same side, with 12 measuring points evenly spaced in the longitudinal direction. The transverse area encompassed a single lane's width, and 10 measurement points were equally spaced. The luminance meter was placed at a longitudinal distance of 60 m from the first row of points, and the lens was 1.5 m above the ground. Figure 5 demonstrates the calculation results of the DIALux light-environment simulation model and its verification. Data in Figure 5b refer to the average luminance of all the transverse points at each longitudinal position. Figure 5 shows that the luminance difference between results obtained from field measurements and those obtained from the model is within 5%, indicating good accuracy of the model.

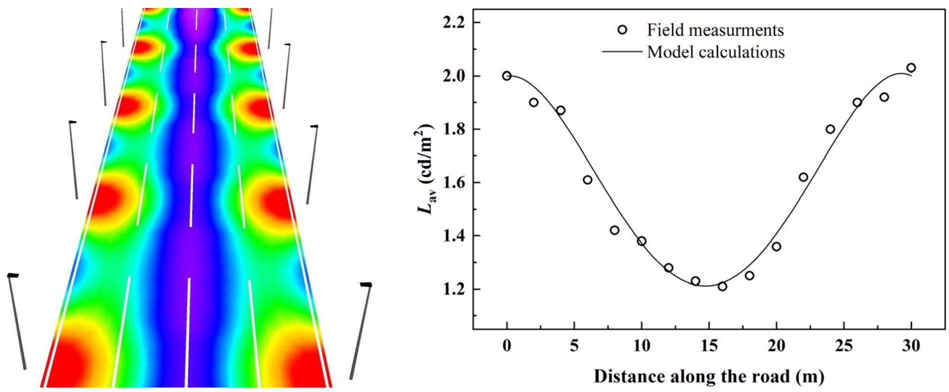

(**a**) (**b**)

Figure 5. Calculation results of the DIALux light-environment simulation model and its verification. (**a**) Luminance distribution on the road surface and (**b**) verification of the model calculation results.

4. Results and Discussion

4.1. Changes in Road Surface Reflective Properties

4.1.1. Effects of the Service Length

The reflective properties of a road surface can be imaged by scattering ellipsoids. The size of the ellipsoid reflects the road surface's reflectivity, while the ellipsoid's flatness reflects its specularity [24]. Figure 6 displays the scattering ellipsoid of the central road area during different service periods, and the data in the figure were representative measurements under identical parallel testing conditions. It becomes apparent that both the size and shape of the ellipsoid change as the service length increases. At the beginning of the road service (0 years), the ellipsoid size is the largest, and its right side is slightly protruding, indicating that the road surface is the most reflective at this time and has a certain degree of specularity. After roughly one year's service, the ellipsoid size declines considerably to around 60% of its initial size, evincing a remarkable decrease in road surface reflectivity. Subsequently, the ellipsoid size exhibited an increase, suggesting a gradual restoration of the reflectivity of the road surface. The reflective capacity of the road surface stabilizes after around 4 years of use. The protrusion on the right side of the ellipsoid was most noticeable at the two-year service point, indicating that the road surface's specularity was at its strongest.

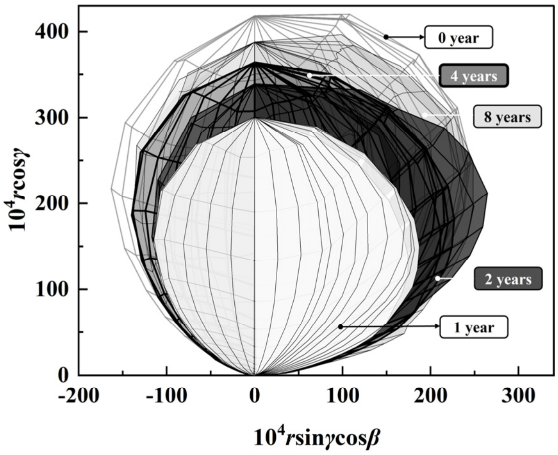

Figure 6. The scattering ellipsoid for different service lengths.

Figure 7 shows the variation of the average luminance coefficient $Q0$ and specular factor $S1$ with road service length, and the data in the figure refer to the mean measurements of several samples under identical parallel testing conditions. Figure 7a demonstrates that as the service length increases, $Q0$ decreases first, then increases, and finally becomes stable. At the beginning of the service, due to the shiny surface of the asphalt road, its reflection ability is strong, and thus, $Q0$ reaches a maximum value over the whole service life, with $Q0$ between 0.075 and 0.08. After about one year of service, a large amount of dust adheres to the road surface, and the oil sheen on the surface of the asphalt road gradually dissipates. At this time, $Q0$ decreases by about 30% compared to the beginning of service, reaching its minimum value (0.06 $\pm$ 0.002) over its entire service period. In the subsequent service, the continuous friction between the vehicle tires and the road surface gradually thinned the asphalt [15], causing the more reflective light-colored aggregates to be continuously exposed, resulting in a gradual increase in $Q0$. Until the road has been in service for 3 to 4 years, $Q0$ reaches a stable stage, and its value was about 80% of that at the beginning of the service. It can be seen that, except at the beginning of the service, the $Q0$ of Chinese urban roads is lower than the $Q0_{standard}$ of R2 and R3 roads. Further comparing the roads of Germany and the United States with Chinese urban roads, it can be found that after 4 years of service, the $Q0$ of German and United States roads can be restored to the level at the beginning of the service [13]. However, due to the large traffic volume, the high proportion of heavy traffic, and the low frequency of road maintenance [27], the recovery capacity of Chinese urban roads is poor, and $Q0$ can only recover to about 80% of that at the beginning of the service after stabilization.

For the design and calculation of road lighting, the current Chinese specifications utilize the R3 standard r-table. The $S1$ ranges for R2 and R3, according to the CIE road surface reflection classification system, are $0.42 \leq S1 < 0.85$ and $0.85 \leq S1 < 1.35$, respectively. However, it can be seen from Figure 7b that the $S1$ of Chinese urban roads varies from 0.6 to 0.83 during its service period, which actually belongs to the R2 roads. Therefore, the standard r-table for R3 roads adopted in the current specification will overestimate the reflectivity and specularity of the road surface.

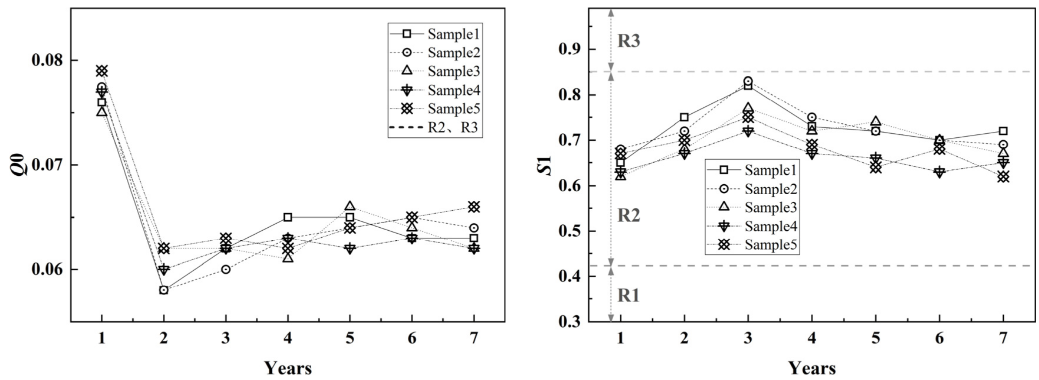

(**a**) $Q0$ (**b**) $S1$

Figure 7. The change of $Q0$ and $S1$ during the service life.

In addition, with the increase in road service length, the $S1$ of Chinese urban roads increases first and then decreases. The $S1$ peaks at about 2 years of service, ranging from 0.7 to 0.83, which is about 1.2 times that at the beginning of service. This is because, during service, the tire rolling can make the road reveal a small amount of aggregate and make the surfaces of these aggregates more polished. The specularity of these aggregate surfaces is strong, resulting in an increase in the specularity of the road surface. Subsequently, under the long-term effects of traffic loads, asphalt on the surface of the road further decreases, and more aggregates are exposed or even lost, leading to a rough road surface and a gradual decrease in $S1$. It should be noted that CIE considers the $S1_{\text{standard,R2}}$ = 0.58 for R2 roads, while the actual specularity of urban roads in Zhejiang province, China, is higher than that of R2 throughout the service period, and thus these roads belong to the R2 road with strong directional reflections. It is clear that a direct application of the R2 r-table will underestimate the specularity of the road surface throughout its service life.

4.1.2. Effects of Area on Road Surface

Figure 8 shows the scattering ellipsoid of different areas on the road surface (served 4 years), and data in the figure were the representative measurements under identical parallel testing conditions. After 4 years of service, the reflective properties of the road surface have basically entered a stable stage. However, Figure 8 shows that the ellipsoid size of the edge, center, and wheel path area on the road surface increases in sequence, indicating sequential increases in the reflectivity of these areas. At the same time, the flatness of the ellipsoid gradually intensifies, indicating that the specularity of these areas increases in sequence.

Furthermore, statistical results of $Q0$ and $S1$ were used to quantitatively analyze the differences in reflective properties of different areas on road surfaces, as shown in Figure 9. Groups 1, 2, and 3 denote the road samples with service lengths of 1~2 years, 3~4 years, and 6~8 years, respectively. As shown in Figure 9a, the variation of $Q0$ with road surface area is consistent with the variation of the ellipsoid with road surface area, i.e., $Q0_{\text{wheel}} > Q0_{\text{center}} > Q0_{\text{curb}}$. Taking Group 1 as an example, compared to $Q0_{\text{curb}}$ and $Q0_{\text{center}}$, $Q0_{\text{wheel}}$ increased by 40% and 14.8%, reaching 0.07. Compared to Groups 1 and 2, Group 3 exhibited a potential increase of up to 62.3% and 32.3% for $Q0_{\text{wheel}}$ compared to $Q0_{\text{curb}}$ and $Q0_{\text{center}}$, respectively, along with a significantly larger dispersion of the data. As the service period lengthens, there is an increasing divergence in the reflective properties of different areas on the road surface.

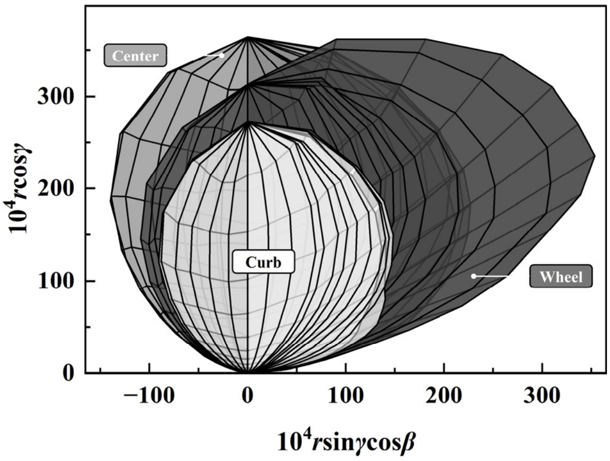

Figure 8. The scattering ellipsoid of different areas.

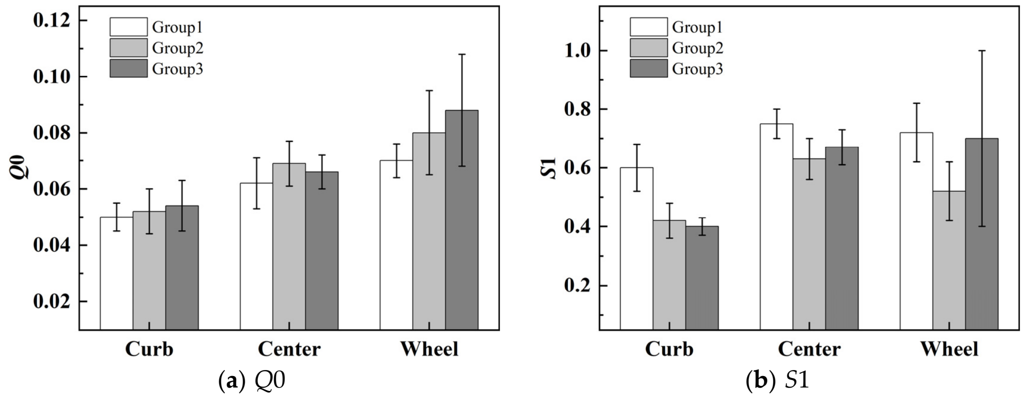

Figure 9. Changes of *Q*0 and *S*1, along with the change of road surface areas.

From Figure 9b, it can be seen that $S1_{wheel}$ and $S1_{center}$ are significantly higher than $S1_{curb}$, and $S1_{wheel}$ has the greatest dispersion, which is consistent with previous research [9]. This can be attributed to the fact that the center of the road surface is more heavily trafficked than the edges, resulting in a greater number of bright glossy aggregates in the center, which are more reflective and have a higher specularity. For the wheel path area with greater traffic load, wheel traces or ruts will make the road surface uneven or even aggregate missing or strip-like grooves, making *S*1 more discrete.

4.1.3. Effects of the Observation Angle

Figure 10 shows the scattering ellipsoid under different observation angles α. α reflects the angular relationship between the driver's attention area, *s*, and the viewpoint height, *h* [23]. Data in Figure 10 were the representative measurements under identical parallel testing conditions. The CIE standard *r*-tables are all based on $\alpha = 1°$ (s = 60~160 m, h = 1.5 m), but with the upgrading of the road classes and the diversification of vehicle types, the α range has been gradually extended to 0.2°~7° (s = 20 m~450 m, h = 1.2 m~2.5 m). Compared to $\alpha = 1°$, the ellipsoid size of $\alpha = 0.2°$ and 0.5° is larger, while the ellipsoid size of α = 2°~7° is significantly reduced. The ellipsoid size under each α differs by a factor of nearly 20, indicating that the reflectivity of the road surface varies greatly. Furthermore, when comparing the shape of each ellipsoid, it can be seen that as α increases, the protrusion of the right side of the ellipsoid decreases slightly, indicating that the specularity of the road surface also decreases.

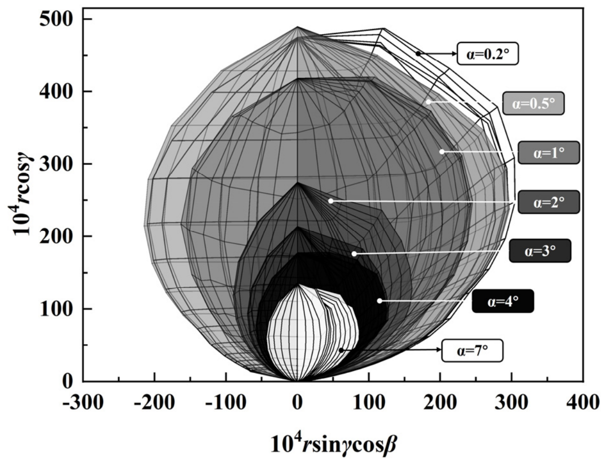

Figure 10. The scattering ellipsoid under different observation angles.

Figure 11 illustrates the alterations of $Q0$ and $S1$ with the α. The data in the figure refer to the mean measurements of several samples under identical parallel testing conditions. It can be seen that Sample 1~Sample 5 all show a similar alteration pattern: as α increases, both $Q0$ and $S1$ gradually decrease, indicating that both the reflectivity and specularity of the road surface decrease. It is noteworthy that the changes in $Q0$ and $S1$ are more substantial when α is $\leq 1°$ and the maximum variations can attain 40% and 20%, respectively. For high-level highways ($s \approx 80$ m~450 m [17]) with high vehicle speed v ($v \geq 80$ km/h) and an extended driver-attention area, it is evident that the reflection conditions of the road surface within the driver's attention area vary considerably.

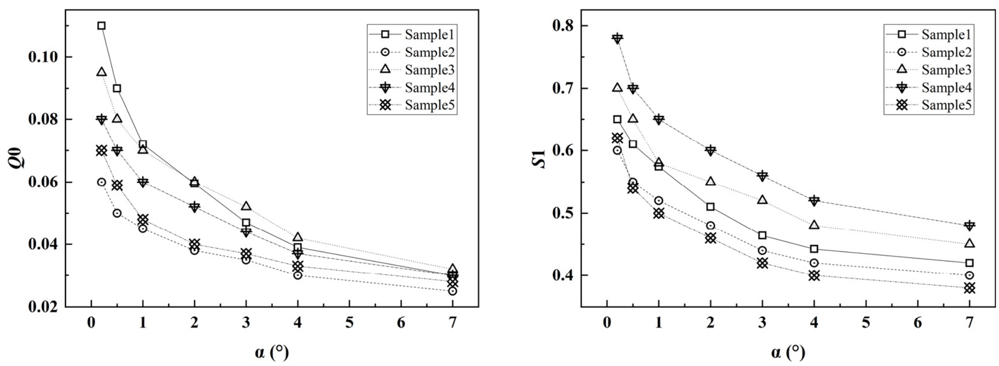

(**a**) $Q0$ (**b**) $S1$

Figure 11. Variation of $Q0$ and $S1$ with observation angle α.

4.2. Changes in Road Lighting Quality during the Full-Service Life

Over the lifespan of a road, changes in the reflective properties of the road surface due to service length and area location will directly impact the road lighting quality, as illustrated in Figure 12. The average luminance (L_{av}) and overall luminance uniformity (U_0) displayed in the figure were calculated via the measured r-tables over the road's entire service life and the CIE standard r-tables for R2 and R3 roads. The actual road lighting quality includes three stages, as shown in Figure 12. Specifically, the first stage refers to the initial period of service (0 years), the second the middle period of service (about 2 years), and the third the stabilization period (after 4 years). The luminance distribution of the road surface in each of these periods is plotted as a 3D greyscale map on the right-hand side of Figure 12.

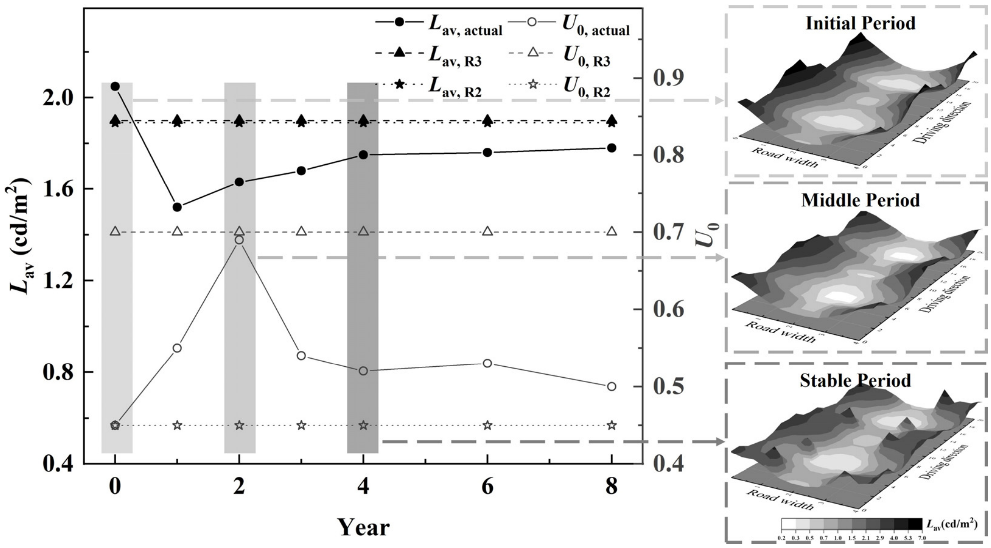

Figure 12. Changes in road lighting quality over the full-service cycle.

The reflection of the road surface is at its highest upon the initial period of service, with a $Q0$ of approximately 0.075~0.08. As a result, the average luminance of the road surface ($L_{av,actual}$) exceeds 2 cd/m^2, which is greater than the luminance calculation results ($L_{av,R2}$, $L_{av,R3}$) attained through the standard *r*-tables for R2 and R3 roads. The 3D greyscale map of road surface luminance distribution reveals that the road surface's high luminance area is located below the lighting fixtures, causing poor luminance uniformity. The $U_{0,\ actual}$ is merely 0.45, which accounts for approximately 65% of $U_{0,R3}$ for the R3 road.

After a year or two of use, as the asphalt starts to lose its shine, the road's reflectivity decreases considerably, leading to a minimal $L_{av,actual}$ throughout its lifespan, typically around 1.55 cd/m^2. This decline coincides with a significant reduction in the luminance contrast between the light and dark areas of the surface, resulting in a maximum $U_{0,\ actual}$ of roughly 0.7. During this period, although the overall luminance uniformity improved significantly, the driver's reaction speed slowed down, and the ability to detect dangerous obstacles was weakened due to the obvious decrease in average luminance, which resulted in a significant increase in the probability of collision accidents.

After 4 years of service, the road lighting quality stabilizes with an increase in $L_{av,actual}$ to 1.8 cd/m^2, slightly lower ($\leq$10%) than that of standard R2 and R3 roads. Notably, differences in luminance between different areas of the road surface emerge at this stage due to prolonged vehicle rolling. The central area of the road, in particular, is prone to forming wheel traces or minor ruts, which create randomly bright areas. Hence, the luminance uniformity undergoes a decline with a $U_{0,actual}$ of approximately 0.5. This value is 30% lower than that of the standard R3 road but 12.5% higher than that of the standard R2 road. Despite the improvement in the average luminance during the stabilization period, the luminance can only be restored to approximately 80% of that at the initial period of service. Additionally, owing to the significant deterioration in luminance uniformity, drivers usually encounter more difficulties detecting obstacles under the actual lighting conditions. Hence, the road is exposed to certain driving safety hazards when it enters the stabilization period.

In summary, for urban roads in Zhejiang, China, significant discrepancies between the actual lighting and that proposed by Chinese specifications often occur when the CIE R3 road standard to design the road lighting is used. This is because the reflective properties of the urban roads in Zhejiang, China, are very different from those of the R3 roads at all service stages. Specifically, the average L_{av} and U_0 for Chinese roads throughout the service are approximately 20% lower than those of R3 roads. This leads to a significant traffic safety risk throughout the entire life cycle of the road. Furthermore, the minimum values of L_{av} and U_0 over the entire service deviate from those of the R3 roads by 35% and 31%, respectively. The analysis showed that the roads in Zhejiang, China, belong to the CIE R2 road and exhibit strong directional reflection. However, directly adopting the R2 road standard for lighting design will result in a 30% lower L_{av} than the recommended value, even though the overall luminance uniformity U_0 meets the standard. Thus, to ensure safety throughout the entire service lifespan of the road, the design criteria for L_{av} should be increased by 35% based on the CIE R2 road standard.

4.3. Lighting Quality under Different Observation Angles

Figure 13 shows the variation in road lighting quality with the observation angle α. In the range of 0.2°~7°, as α increases, the average luminance L_{av} decreases rapidly, and the overall luminance uniformity U_0 and longitudinal luminance uniformity U_L increase gradually. Psychological evidence shows that drivers tend to perceive the road further ahead as being brighter and safer [28]. This is because when drivers look at the road ahead, α decreases as the line of sight extends. Notably, when $\alpha \geq 4°$, L_{av} is less than 0.78 cd/m^2, which is about 50% of that for α = 1°. This is in line with the results of the European SURFACE project [23] ($L_{av,\alpha=5°} \approx 50\% L_{av,\alpha=1°}$) and shows that there is no significant difference between urban roads in the Zhejiang region of China and roads in European countries in terms of the influence of α on the road lighting.

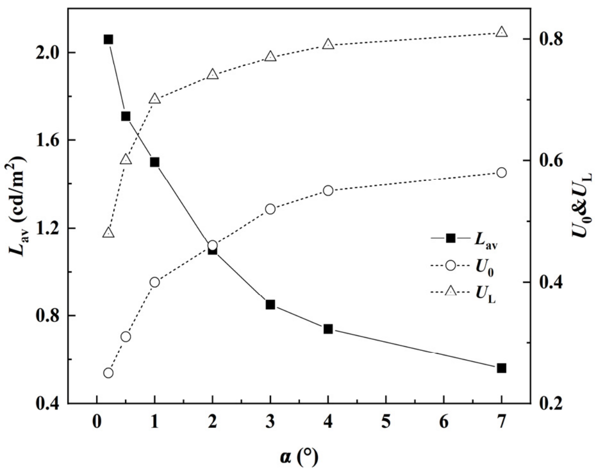

Figure 13. Changes in the lighting quality with observation angles.

For urban expressways (i.e., roads that can facilitate fast traffic movement and with the characteristics of long distances and high traffic volumes), major roads (i.e., roads that connect the primary sub-districts of the city, incorporating both motorized and non-motorized forms of transport segregation), and other high-level urban roads, the observation angle is often much less than 1° because the vehicle speed can reach 60~100 km/h on these roads. Under the same road lighting conditions, the L_{av} perceived by the driver will be about 40% higher than that at α = 1°, but the U_0 and U_L will be 30% lower or more. Suppose road lighting is still designed according to the normative standard (α = 1°). In that case, drivers will be continuously exposed to high luminance but low luminance uniformity, i.e., they will be exposed to large and high-frequency light and dark stimuli for long periods of time, leading to a significant reduction in their reaction speed and ability to detect obstacles [29], thus decreasing driving safety [30]. Therefore, for high-level urban roads such as urban expressways and major roads, it is recommended that the design criteria for U_0 in the current road lighting specification should be increased by 40%, i.e., reach 0.65.

On collector roads (i.e., roads that combine with major roads to form a network for the collection and distribution of traffic) and local roads (i.e., roads that connect the collector roads and residential roads), vehicles usually travel at relatively slow speeds, and the height of the driver's viewing point h is usually high. For example, for a truck driver, h is

2 m or higher, and the corresponding α often reaches more than 4°. If the road lighting is still designed on the basis of α = 1°, it may result in insufficient L_{av} (around 45% lower), making it difficult for drivers to detect road obstacles clearly, thus leading to significantly higher traffic safety risks. Therefore, it is recommended to increase the design criteria of L_{av} in the current road lighting specification by 45% for collector roads, local roads, and other roads.

5. Conclusions

The urban asphalt road in Zhejiang Province, China, is an R2 road that exhibits low resilience and strong directional reflection. The average luminance coefficient $Q0$ reaches a maximum value (0.077 $\pm$ 0.002) and a minimum value (0.06 $\pm$ 0.002) at the beginning of the road service (within 3 months) and around 1 year, respectively. After four years of service, $Q0$ stabilizes at about 80% of its initial value. The maximum value of the specular factor $S1$ (0.07–0.83) is reached after two years of road service, which is about 1.2 times that at the beginning of service or during the stabilization period. The $Q0$ varies in different areas of the road surface, with $Q0_{\text{wheel}}$ being larger than $Q0_{\text{center}}$ and $Q0_{\text{curb}}$. Both $S1_{\text{wheel}}$ and $S1_{\text{center}}$ are significantly larger than $S1_{\text{curb}}$, and the dispersion of the $S1_{\text{wheel}}$ is the largest due to the irregular reflections caused by rutting.

The average luminance L_{av} and the overall luminance uniformity U_0 correspond well with the $Q0$ and $S1$, respectively. The minimum L_{av} was observed before and after one year of road usage when the reflective capacity of the road surface was the weakest. During this period, $Q0$ was reduced by approximately 30% compared to its initial value. The minimum U_0 was recorded after around four years of road service. Throughout the entire lifespan of the road, the $L_{\text{av,actual}}$ and $U_{0,\text{actual}}$ during the most adverse period, are approximately 35% and 31%, respectively, lower than those of the R3 road standard proposed by the current Chinese specification. If the R3 road standard is used directly for the lighting design, the road will be exposed to traffic safety risks during any period of service.

As the observation angle α increases, L_{av} descends hastily while U_0 and U_L elevate gradually. For urban expressways and major roads with vehicle speeds of 60 km/h to 100 km/h, the actual α of the driver is often less than 1°. If the road lighting is designed according to the current Chinese specification's standard *r*-table (where α = 1°), it can result in consistently high luminance and low luminance uniformity, bringing about a safety hazard. On collector roads and local roads, as well as other lower-speed roads, the actual α of truck drivers is much larger than 1°, which makes it difficult to clearly identify obstacles due to insufficient road surface luminance.

Taking into account the impact of road surface reflectiveness on lighting quality throughout the life of the road, it is recommended that urban asphalt roads in Zhejiang Province, China, should adopt the R2 standard and increase the design standard for the average luminance, L_{av}, by 35~45%. Furthermore, for urban expressways, major roads, and high-level roads, it is necessary to increase the design standard of overall luminance uniformity U_0 by an additional 40%.

The major findings reveal the long-term variation of reflective properties of the urban road surface and potential impacts on driving safety. Meanwhile, the proposed study also provides scientific references for the design of lighting for urban roads in China, thus paving the way for a traffic-safe, sustainable city.

Author Contributions: C.Z.: conceptualization; data curation; formal analysis; investigation; methodology; software; validation; visualization; writing—review and editing. C.L.: conceptualization; data curation; formal analysis; investigation; methodology; software; writing—original draft. L.Y.: funding acquisition. C.K.: formal analysis; methodology; project administration; supervision; writing—review and editing. M.W.: methodology; visualization. Z.H.: supervision. K.W.: conceptualization; funding acquisition; project administration; resources; supervision; writing—review and editing. All authors have read and agreed to the published version of the manuscript.

Funding: This work was supported by the Ningbo Transportation Science and Technology Plan Project [grant number 202113]; the Science and Technology Project of Zhejiang Provincial Department of Transport [grant number 2022-GCKY-02]; and the Artificial Intelligence Key Technologies R & D Program of Hangzhou [grant numbers 2022AIZD0057, 2022AIZD0102].

Institutional Review Board Statement: Not applicable.

Informed Consent Statement: Not applicable.

Data Availability Statement: Data will be made available upon request.

Conflicts of Interest: Cheng Kang was employed by the company China Railway First Survey and Design Institute Group Co., Ltd. The remaining authors declare that the research was conducted in the absence of any commercial or financial relationships that could be construed as a potential conflict of interest.

References

1. *CIE 93:1992*; Road Lighting as an Accident Counter-Measure. CIE Central Bureau: Vienna, Austria, 1992.
2. Elvik, R. Meta-Analysis of Evaluations of Public Lighting as Accident Countermeasure. *Transp. Res. Rec.* **1995**, *1485*, 112–123.
3. *CIE 66:1984*; Road Surfaces and Lighting (Joint Technical Report CIE/PIARC). CIE Central Bureau: Vienna, Austria, 1984.
4. *CIE 144:2001*; Road Surface and Road Marking Reflection Characteristics. CIE Central Bureau: Vienna, Austria, 2001.
5. *CJJ 45—2015*; Standard for Lighting Design of Urban Road. Ministry of Housing and Urban-Rural Development of the People's Republic of China: Beijing, China, 2015.
6. *JTG/T D70/2-01-2014*; Guidelines for Design of Lighting of Highway Tunnels. Ministry of Transport of the People's Republic of China: Beijing, China, 2014.
7. Zhang, Q.; Li, X. Development and Evolution of Asphalt Pavement Structural Design Methods in China over the Past 70 Years. *J. China Foreign Highw.* **2019**, *39*, 30–38.
8. Chain, C.; Lopez, F.; Verny, P. Impact of Real Road Photometry on Public Lighting Design. In Proceedings of the 26th Session of the CIE, Beijing, China, 4–11 July 2007; pp. 4–11.
9. Gidlund, H.; Lindgren, M.; Muzet, V.; Rossi, G.; Iacomussi, P. Road Surface Photometric Characterisation and Its Impact on Energy Savings. *Coatings* **2019**, *9*, 286. [CrossRef]
10. Wood, J.M. Nighttime Driving: Visual, Lighting and Visibility Challenges. *Ophthalmic Physiol. Opt.* **2020**, *40*, 187–201. [CrossRef] [PubMed]
11. Beyer, F.R.; Ker, K. Street Lighting for Preventing Road Traffic Injuries. *Cochrane Database Syst. Rev.* **2009**, CD004728. [CrossRef] [PubMed]
12. van Bommel, W. *Road Lighting: Fundamentals, Technology and Application*; Springer: Berlin/Heidelberg, Germany, 2015; ISBN 9783319114668.
13. Rice, J.; Hoon Kim, Y.; Sun, Z.; Mohsen, J.P. Evaluation of Light Reflectiveness of Modern Pavement: Standard Tungsten Incandescent and LED. *J. Transp. Eng. Part B Pavements* **2020**, *146*, 04020007. [CrossRef]
14. Bodmann, H.W.; Schmidt, H.J. Road Surface Reflection and Road Lighting: Field Investigations. *Light. Res. Technol.* **1989**, *21*, 159–170. [CrossRef]
15. Ylinen, A.; Puolakka, M.; Halonen, L. Road Surface Reflection Properties and Applicability of the R-Tables for Today's Pavement Materials in Finland. *Light Eng.* **2010**, *18*, 78–90.
16. Wang, S.; Yu, D.; Kwan, M.P.; Zheng, L.; Miao, H.; Li, Y. The Impacts of Road Network Density on Motor Vehicle Travel: An Empirical Study of Chinese Cities Based on Network Theory. *Transp. Res. Part A Policy Pract.* **2020**, *132*, 144–156. [CrossRef]
17. Jo, D.; Lee, S.; Lee, Y. The Effect of Driving Speed on Driver's Visual Attention: Experimental Investigation. In Proceedings of the Lecture Notes in Computer Science (Including Subseries Lecture Notes in Artificial Intelligence and Lecture Notes in Bioinformatics), Macau, China, 4–7 December 2012; Springer: Berlin/Heidelberg, Germany, 2014; Volume 8532, pp. 174–182.
18. Liu, W. *Automotive Design*; Tsinghua University Press: Beijing, China, 2001.
19. Kamp, I. The Influence of Car-Seat Design on Its Character Experience. *Appl. Ergon.* **2012**, *43*, 329–335. [CrossRef] [PubMed]
20. Wang, J.S.; Knipling, R.R.; Blincoe, L.J. The Dimensions of Motor Vehicle Crash Risk. *J. Transp. Stat.* **1999**, *2*, 19–43.
21. Gibbons, R.B.; Adrian, W.K. Influence of Observation Angle on Road Surface Reflection Characteristics. *J. Illum. Eng. Soc.* **1997**, *26*, 139–149. [CrossRef]
22. Strbac-Hadzibegovic, N.; Strbac-Savic, S.; Kostic, M. A New Procedure for Determining the Road Surface Reduced Luminance Coefficient Table by On-Site Measurements. *Light. Res. Technol.* **2019**, *51*, 65–81. [CrossRef]
23. Muzet, V.; Bernasconi, J.; Iacomussi, P.; Liandrat, S.; Greffier, F.; Blattner, P.; Reber, J.; Lindgren, M. Review of Road Surface Photometry Methods and Devices—Proposal for New Measurement Geometries. *Light. Res. Technol.* **2021**, *53*, 213–229. [CrossRef]
24. Dumont, E.; Paumier, J.-L. Are Standard Tables R Still Representative of the Properties of Road Surfaces in France? In Proceedings of the 26th CIE International Symposium on Road Surface Photometric Characteristics, Beijing, China, 4–11 July 2007; pp. 4–11.
25. *GB/T 11147-2010*; Standard Practice for Sampling Bituminous Materials. Standard Press of China: Beijing, China, 2011.
26. *GBT 5700-2008*; Lighting Measurement Methods. Standard Press of China: Beijing, China, 2008.

27. Huang, Q.; Shi, J. Optimizing Work Zones for Two-Lane Urban Road Maintenance Projects. *Tsinghua Sci. Technol.* **2008**, *13*, 644–650. [CrossRef]
28. Fotios, S.; Unwin, J.; Farrall, S. Road Lighting and Pedestrian Reassurance after Dark: A Review. *Light. Res. Technol.* **2015**, *47*, 449–469. [CrossRef]
29. Kimura, M.; Hirakawa, S.; Uchino, H.; Motomura, H.; Jinno, M. Energy Savings in Tunnel Lighting by Improving the Road Surface Luminance Uniformity—A New Approach to Tunnel Lighting. *J. Light Vis. Environ.* **2014**, *38*, 66–78. [CrossRef]
30. Kang, C.; Lin, G.; Ye, L.; Zhang, C.; Huang, Z.; Wu, K. Influence of Luminance and Luminance Longitudinal Uniformity of Tunnel Lighting on Drivers' Comprehensive Visual Performance. *Tunn. Undergr. Sp. Technol.* **2023**, *140*, 105282. [CrossRef]